Twelfth International Conference on Computational Fluid Dynamics (ICCFD12), Kobe, Japan, July 14-19, 2024

Wall-Modeled Large Eddy Simulation on Heat Transfer in a Nasal Cavity to 14-Generation Respiratory Tract

Xinlei Huang* and Huining Cui*
Corresponding author's e-mail: xinlei.huang@student.uts.edu.au
* Faculty of Engineering and Information Technology, University of Technology Sydney, Sydney, New South Wales 2007, Australia

Abstract: Athletes in cold environments face significant health risks due to cold, dry air inhalation, often leading to respiratory injuries. Prior research has mainly focused on lung airway heat transfer, overlooking the broader respiratory tract. Addressing this gap, our research comprehensively assesses the entire respiratory system, from nasal and oral cavities to the 13th generation of lung airways. Utilizing advanced Computational Fluid Dynamics (CFD), including Large Eddy Simulation (LES) integrated with an algebraic wall-modeled LES (WMLES) subgrid-scale model, we simulate heat transfer within the human lung during exhalation. This innovative approach reveals complex dynamics of respiratory thermoregulation in cold environments, providing a detailed view of temperature, heat flux, and static pressure profiles across the respiratory tract. These insights enhance understanding of the physiological response to cold air exposure, which is crucial for athlete health and performance. The study illuminates the complexities of cold-induced respiratory challenges and lays the groundwork for developing more effective preventive strategies and optimizing athletic performance in cold conditions.

Keywords: Large Eddy Simulation, Heat Transfer, Human Respiratory System, Health

1 Introduction

Exhalation is a crucial component of the body's thermoregulatory processes, where the cooling of exhaled air aids in heat conservation—an aspect crucially highlighted in prior research [1, 2]. Despite the expansive application of computational fluid dynamics [3] enhancing our comprehension of physiological phenomena [4] of respiratory dynamics, the full cycle of air movement, particularly during exhalation, remains less explored.

Respiration injuries have received significant attention due to their severity and rapid progression, especially those resulting from exposure to extreme temperatures [5-7]. Conversely, the specific dynamics of exhalation in cold climates have not been as thoroughly investigated despite their importance in maintaining thermal homeostasis and protecting lung tissue. Earlier studies have predominantly focused on the thermal and moisture exchanges during inhalation, providing extensive insights into the air conditioning functions of [8, 9] as well as pressure drops [10, 11] within the nasal cavity, heat and mass transfer within the lung [12]. However, there is currently a significant lack of information regarding thermal injuries within the pulmonary system [13], particularly during exhalation. Athletic performance impairments due to cold exposure vary by activity and muscle group, with significant reductions in maximal wrist flexion force at 5°C [14] and leg extensor power at 15°C compared to 25°C [15], but climbing-specific tasks show improved endurance and unchanged strength at 10°C [16]. Therefore, studying the effects of ambient temperatures of 5°C and 25°C on the human respiratory tract is crucial, as these temperatures are known to impact athletic performance significantly. This research aims to fill this gap by simulating the exhalation phase under two specific cold conditions,

at 5℃ and 25℃, using advanced LES turbulence modeling. By doing so, it seeks to provide a detailed understanding of the interaction between airflow and heat transfer. The present study extends our previous investigation [17] to the exhalation phase in cold environments, complementing the initial focus on inhalation. This analysis will not only deepen our knowledge of respiratory thermodynamics but also contribute to developing effective strategies to mitigate the respiratory challenges athletes face in cold environments.

Such insights are essential for improving athletic performance and safety in outdoor sports, offering a foundation for preventive measures and interventions tailored to cold exposure. This study's findings could lead to enhanced guidelines for athletes training in various temperature conditions, ensuring their well-being and optimizing physiological responses to cold air.

2 Methodology

2.1 Computational Model of the Respiratory Tract

This research presents the development of a complex computational model of the human respiratory tract. For a detailed description of the geometric processing techniques utilized in this model, we direct readers to our prior research [12]. As depicted in Figure 1 (a), the model captures the complex anatomical structures of the respiratory system. It employs a sophisticated polyhedral mesh scheme, featuring four boundary layers. The density of the mesh is adapted based on local geometric scales and variations in turbulence intensity, as illustrated in Figure 1 (b). Ethical considerations were stringently upheld throughout the study, with the Human Research Ethics Committees at the University of Technology Sydney approving the use of human computed tomography scans for this research (ETH23-8670).

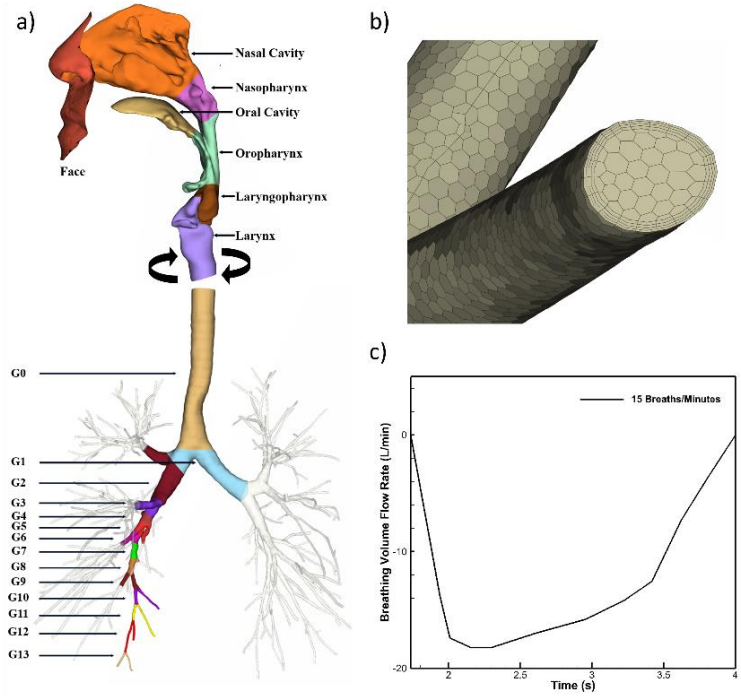

Figure 1: Displays (a) visualization of the respiratory tract model with a schematic outlining the segmented anatomical parts from the nasal cavity to Generation 13 airways, (b) visualization of the polyhedral mesh applied at the bronchial outlet, and (c) realistic volume flow rate boundary condition applied at the inlet.

2.2 Boundary Conditions and Material Properties

Inlet velocity features a realistic velocity profile by multiplying the experimentally measured volume flow rate [18] with the nostril inlet area, as shown in Figure 1 (c). The outer wall temperatures are maintained at 310.15 K. The outlet pressure is set to 0 Pa, and wall conduction is modelled by 1-layer shell conduction with a 5 mm wall thickness. The initial conditions for temperature, pressure, and velocity fields are set based on the state at the end of a pre-simulated 0.43s inhalation phase. The simulation then continues from 0.43 to 1 second to capture the dynamics of the subsequent exhalation phase. At an ambient environment of 25°C, cool air has a temperature of 298.15 K, a density of 1.184 kg/m³, thermal conductivity of 0.025 W/m·K, dynamic viscosity of 1.849×10^-5 Pa·s, and specific heat of 1007.5 J/kg·K. Conversely, at 5°C, the cool air temperature drops to 278.15 K, with a density of 1.270 kg/m³, thermal conductivity of 0.024 W/m·K, dynamic viscosity of 1.748×10^-5 Pa·s, and specific heat of 1005.7 J/kg·K.

2.3 Governing Equations

In this investigation, we adopted the LES technique, specifically integrated with the algebraic WMLES subgrid-scale model, to accurately model the dynamic behavior of airflow within the respiratory tract. LES is renowned for its computational prowess in capturing large-scale turbulent structures, while effectively parameterizing the smaller, unresolved scales. This method strikes a sophisticated balance between the comprehensive detail offered by Direct Numerical Simulation and the computational efficiency of Reynolds-averaged Navier-Stokes simulations. The WMLES model stands out for its innovative application of a wall function that adeptly calculates fluid dynamics characteristics near the boundary layers. This function substantially decreases the computational demands typically required for detailed resolution of near-wall airflow phenomena, yet it preserves the necessary accuracy for analyzing significant turbulent structures.

Central to our study are the fundamental principles of fluid dynamics, as articulated through the Navier-Stokes equations, which comprise continuity, momentum, and energy conservation laws. The continuity equation (Eq. 1) ensures mass conservation across the fluid domain, quantifying the mass exchange within a defined control volume. The momentum equation (Eq. 2) delineates the complex balance between pressure forces and viscous and inertial effects, which are important for a comprehensive understanding of fluid motion. Lastly, the energy equation (Eq. 3) is instrumental in assessing thermal dynamics, including mechanisms of convection, conduction, and heat generation. This equation is vital for describing the temperature fluctuations that occur within turbulent flows, thereby providing a deeper insight into thermal transport phenomena in respiratory airflow.

Continuity equation:

$$\frac{\partial \rho}{\partial t} + \nabla \cdot (\rho \boldsymbol{u}) = 0 \tag{1}$$

Where ρ is the fluid density, t is time, and $\boldsymbol{u}$ is fluid velocity vector.

Momentum equation:

$$\frac{\partial \rho \boldsymbol{u}}{\partial t} + \nabla \cdot (\rho \boldsymbol{u}\boldsymbol{u}) = -\nabla p + \nabla \cdot (\bar{\bar{\tau}}) + \rho \boldsymbol{g} \tag{2}$$

Where p is static pressure, $\bar{\bar{\tau}}$ is stress tensor, and $\boldsymbol{g}$ is gravitational acceleration vector.

Energy equation:

$$\frac{\partial \rho E}{\partial t} + \nabla \cdot (\boldsymbol{u}(\rho E + p)) = \nabla \left(k_{eff} \nabla T - \sum_j h_j \boldsymbol{J}_j + \left(\bar{\bar{\tau}}_{eff} \cdot \boldsymbol{u} \right) \right) \quad (3)$$

Where E is energy, k_{eff} is effective conductivity, T is temperature, h_j is the enthalpy of species j, $\boldsymbol{J}_j$ is diffusion flux of species j, and $\bar{\bar{\tau}}_{eff}$ is the effective stress tensor.

The eddy viscosity employed in the LES is derived using the optimized equations from the algebraic WMLES, where the turbulence viscosity is determined as follows [19]:

$$\upsilon_t = min\left[(\kappa d_w)^2, \left(C_{Smag} \Delta \right)^2 \cdot S \cdot \left\{ 1 - exp\left[-\left(\frac{y^+}{25} \right)^3 \right] \right\} \right] \quad (4)$$

Where κ is a model constant that equals 0.4187, d_w is wall distance, C_{Smag} is a model constant that equals 0.2, S is strain rate, and $y^+$is normal to the wall inner scaling.

2.4 Validation and Verification Assessment

The numerical methodology employed in this study has been rigorously validated and verified in our previous works, focusing on multiple key performance metrics. These include the accuracy of the pressure field [12], mass transfer rates and velocity field dynamics [20, 21], and thermodynamic properties [12, 17].

3 Results and Discussion

3.1 Volume Temperature

In this study, the airway volume temperature, representing the volume-weighted average static temperature, elucidates the temperature dynamics throughout the entire respiratory tract when breathing out into ambient air. As shown in Figure 1, initially, the respiratory tract's air starts at a lower temperature and begins to warm up due to the exhalation of warmer air from the lungs into cooler ambient air. The rate of temperature increase is significantly faster when exhaling within the ambient air at 278.15 K (which means the ambient air at 278.15 K was inhaled during inspiration) compared to the warmer ambient air at 298.15 K. This suggests that the heat transfer between the airway walls and the exhaling air is more efficient at lower temperatures.

Throughout the timeframe shown, from approximately 0.44 seconds to 0.6 seconds, the air temperature in both scenarios exhibits a consistent rise. After 0.6 seconds, both temperature profiles stabilize at the same level, which is why the graph displays data only up to this point. This approach is consistent across all profile graphs that show less than one second of data in subsequent sections; the latter part of the data is omitted to illustrate the trends more clearly within the profiles. In the graph, the temperature curve for exhalation into ambient air at 298.15 K nearly plateaus as it approaches the airway wall temperature, indicating an approaching equilibrium state.

Figure 3 presents a detailed visualization of velocity streamlines, color-coded to reflect volume temperature changes over time, spanning from 0.45 to 1 second. In the exhalation phase depicted in the figure, the transition from cooler to warmer temperatures within the respiratory tract's model demonstrates the efficiency of heat exchange during exhalation. Initially, at 0.45 seconds, the thermal streamlines begin to display a uniform warming trend throughout the airway tree, a stark contrast to the cooler states observed during inhalation. As exhalation proceeds, the figures from 0.47 seconds to 0.51 seconds exhibit a steady increase in temperature, signifying a thermal recovery towards the body's baseline internal temperature. Notably, the upper segments of the respiratory tract, including the trachea

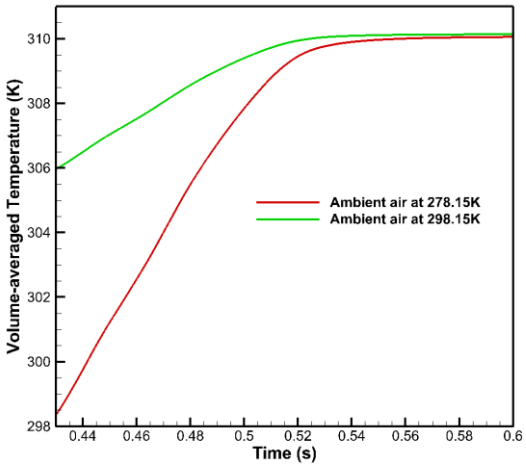

Figure 2: Temporal changes of volume-weighted average temperature in the respiratory tract when inhaling air at 298.15 and 278.15 K.

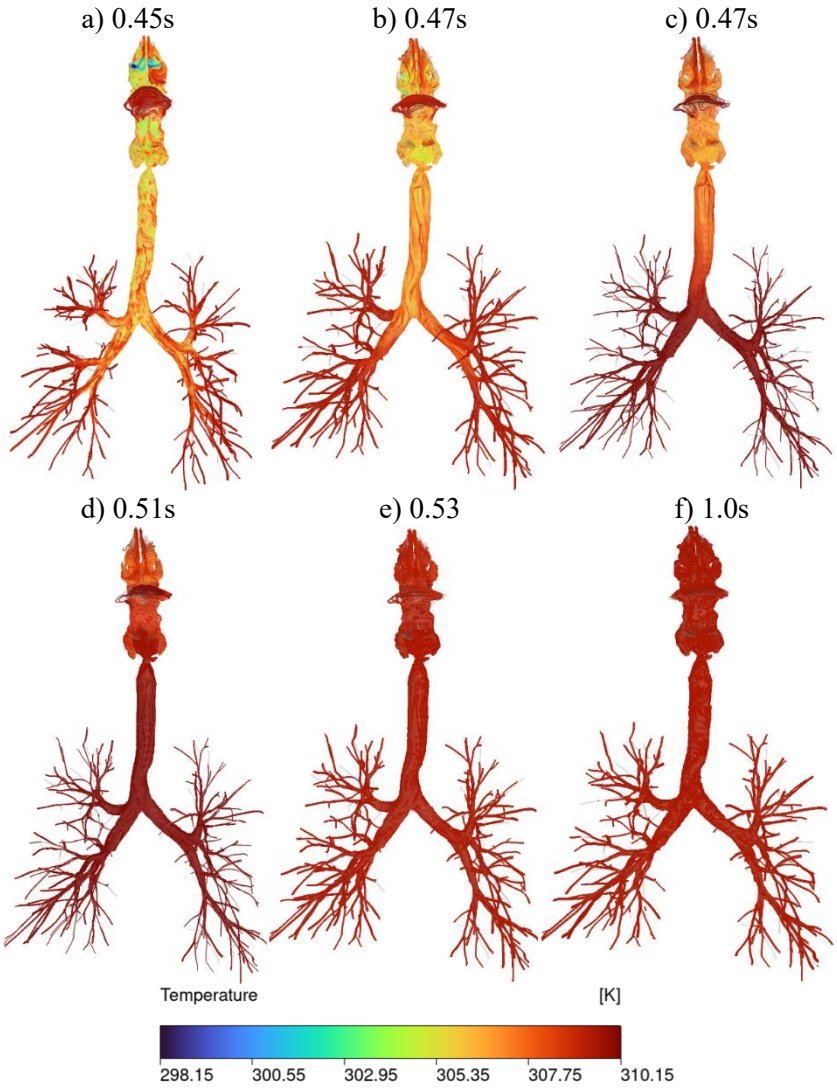

Figure 3: Displays the velocity streamlines colored based on local volume temperature in the respiratory tract from 0.45 to 1 second.

and the major bronchi, show significant warming, highlighted by the shift in colors towards the warmer end of the spectrum. This suggests an efficient warming of air as it moves upwards, mixing with the relatively warmer ambient air entering the system. From 0.51 seconds onward, the temperature appears to nearly stabilize across the entire airway structure, nearing equilibrium close to the expected physiological norm. The images at 0.53 seconds and 1.0 seconds particularly illustrate this stabilization, where the entire respiratory tract appears in shades indicating temperatures close to normal body temperature. This suggests that by the end of the exhalation phase, the airway has efficiently regained much of the heat initially lost to the cooler inhaled air.

The progression of these thermal changes highlights the respiratory tract's capability to modulate its internal environment in response to external temperature variations, effectively managing heat transfer through mechanisms that might involve both convective heat transfer and conductive interactions with the airway walls. This dynamic heat exchange is crucial for maintaining the protective and functional integrity of the respiratory system under varying ambient conditions.

3.2 Airway Wall Surface Static Temperature

The airway wall surface temperature plays a crucial role as the interface between the respiratory air and the adjacent wall. In this study, the human airway wall is modeled as a 5 mm thick, single-layered shell initially at a stable temperature of 310.15 K. During the exhalation phase, the internal air, previously cooled by inhalation of external air at lower temperatures, engages in a dynamic heat exchange process with the warmer airway walls. This interaction, governed by conduction and convection mechanisms, facilitates a gradual increase in the wall surface temperature. According to thermodynamic principles, this warming process is expected as the exhaled air, carrying heat from deeper within the body, transfers energy back to the airway walls, thereby elevating their temperature and restoring them closer to physiological norms.

Figure 4 graphically represents the changes in airway wall surface temperatures during the exhalation phase for various segments of the respiratory tract, illustrating a progressive warming trend as the cooler inhaled air is reheated by the body's internal mechanisms. Specifically, Figures 4 (a) and (b) depict the temperature dynamics within different regions of the upper airway while exhaling air initially inhaled at 278.15 K and 298.15 K, respectively. The graphs show a marked increase in temperature across all regions—nasal cavity, nasopharynx, oropharynx, laryngopharynx, and larynx—commencing around the 0.44-second mark. Notably, the nasal cavity, which experiences the coldest inhaled air temperatures, shows the most significant rise, suggesting a robust heat exchange as the exhaling air ascends through the respiratory tract. In Figures 4 (c) and (d), the focus shifts to the temperature profiles across various generations of the lower airway during exhalation. These figures illustrate a sequential warming trend through generations G0 to G13. As the air moves through these lower airway generations, it undergoes progressive warming, indicating effective heat conduction from the airway walls and possibly the surrounding tissues. This effect is more pronounced in the earlier generations (G0 to G6), with a smoother transition observed in later generations (G7 to G13), where the temperature profiles gradually converge towards a uniform warmth, reflective of the body’s internal temperature nearing physiological norms.

The temperature recovery in the airway wall surfaces during exhalation highlights the body's efficient thermoregulatory mechanisms. Through conduction and the natural warming capabilities of the body, the airway walls serve as a critical interface for reheating the exhaling air, ensuring that the internal environment is maintained at a stable and suitable temperature. This dynamic is crucial for protecting the respiratory tract against thermal stress and maintaining overall respiratory health.

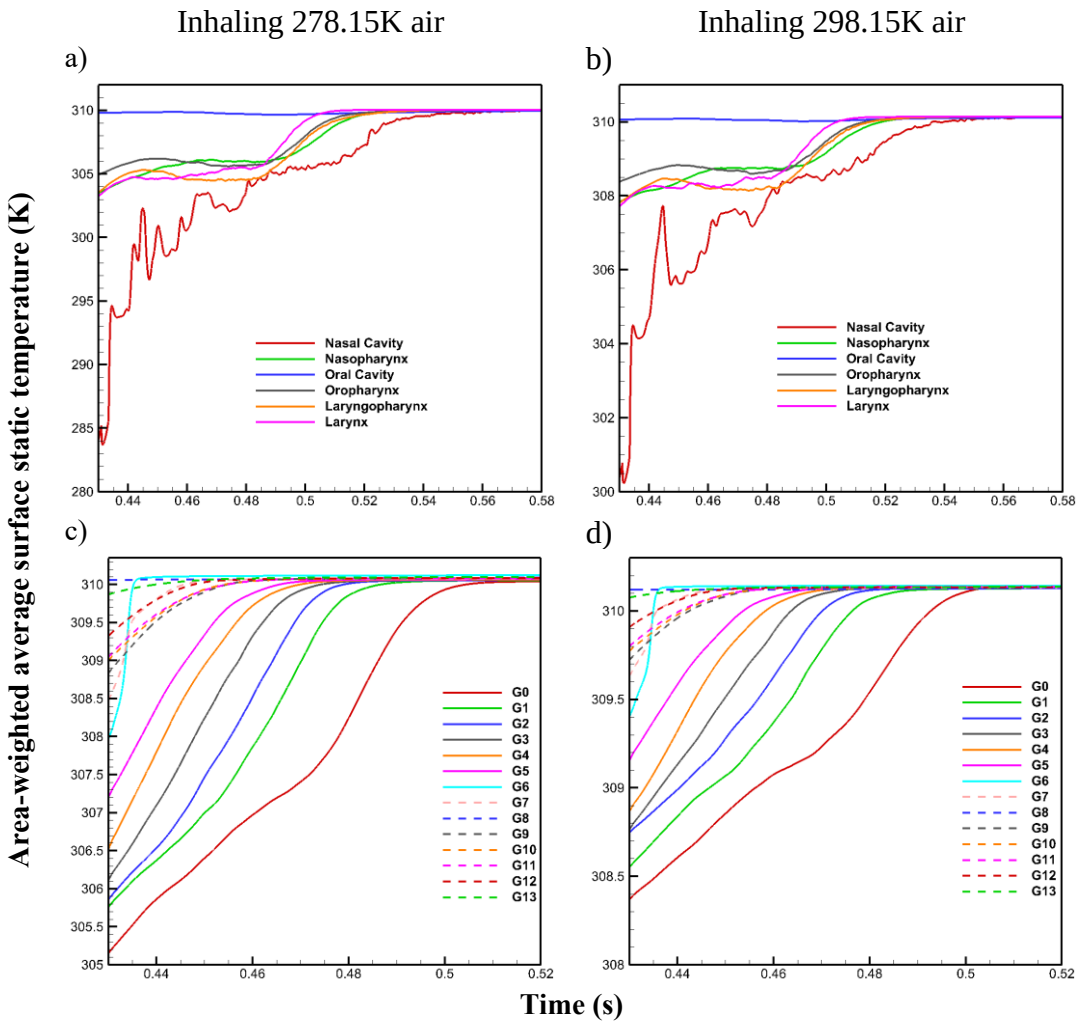

Figure 4: Airway wall surface temperature (K) changes during exhalation: (a) Upper airway at 278.15, (b) Upper airway at 298.15 K, (c) Lower airway at 278.15K, (d) Lower airway at 298.15 K.

3.3 Airway Wall Surface Heat Flux

In the context of exhalation, the airway wall surface heat flux becomes a critical indicator of the heat transfer efficiency between the warmed airway walls and the cooler exhaling air. During exhalation, the previously cooled air, due to the inhalation of cooler external air at temperatures of 298.15 K and 278.15 K, is reheated. This reheating initiates a reverse heat transfer process, predominantly governed by conduction and convection mechanisms. According to thermodynamic principles, this process leads to an increase in wall surface heat flux as the warmer airway walls transfer heat to the cooler exhaling air, thereby reducing the temperature gradients established during inhalation.

Figure 5 details the dynamic variations in wall surface heat flux during the exhalation phase for different regions of the respiratory tract, illustrating the thermal energy transfer as the previously cooled inhaled air is reheated by the body during exhalation. Specifically, Figures 5 (a) and (b) show the heat flux profiles in the upper airway when exhaling previously inhaled air at 278.15 K and 298.15 K, respectively. There is a rapid decrease in heat flux from a high initial value, reflecting the intense initial heat transfer needed to warm the cooler inhaled air. As exhalation continues, the heat flux steadily declines as the temperature difference between the air and the airway walls decreases, leading to less energy transfer required. In Figures 5 (c) and (d), the focus is on the lower airway generations during

exhalation. These figures demonstrate a more gradual decline in heat flux across the generations, from G0 to G13. This trend indicates a progressive decrease in the energy transfer as the exhaling air moves through the airway, warming up and reducing the temperature gradient with each successive generation. This overall decrease in heat flux during exhalation illustrates the efficiency of the body's heat exchange mechanisms, where the respiratory tract effectively uses its structural warmth to elevate the temperature of the exhaling air, reducing the thermal energy transfer as the air's temperature approaches that of the airway walls. This process is critical for maintaining thermal homeostasis within the respiratory system during the breathing cycle.

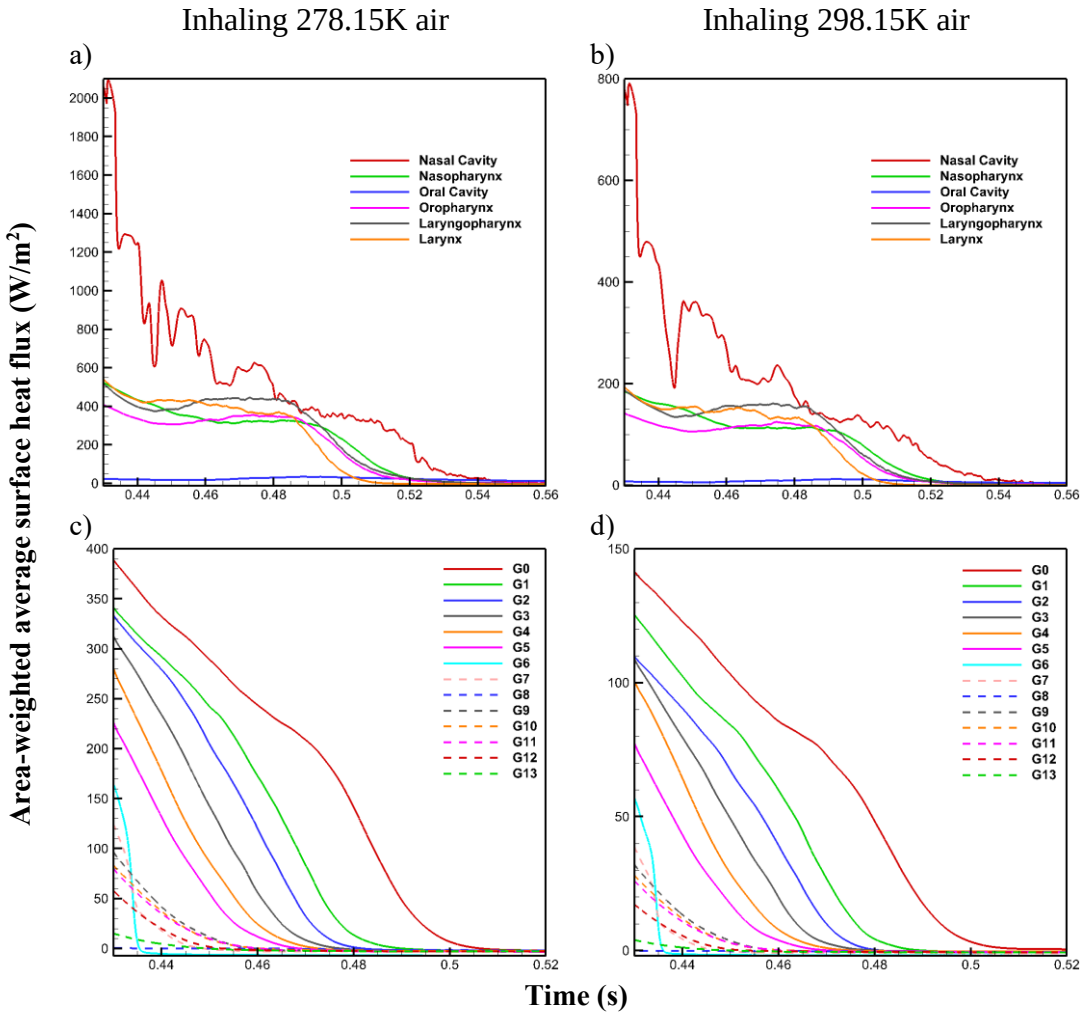

Figure 5: Wall surface heat flux (W/m2) changes during exhalation: (a) Upper airway at 278.15, (b) Upper airway at 298.15 K, (c) Lower airway at 278.15K, (d) Lower airway at 298.15 K.

3.4 Airway Wall Static Pressure

The airway wall static pressure is influenced by the force exerted per unit area by the moving air against the airway walls, which inherently changes as the air velocity and direction vary during exhalation. According to principles of fluid dynamics, this results in fluctuations in static pressure, typically leading to a decrease as air moves from regions of higher to lower resistance, facilitating the air's journey back to the atmospheric environment. This dynamic is crucial for understanding the biomechanical behavior of the respiratory system during the breathing cycle, particularly how it efficiently manages air expulsion

to maintain respiratory homeostasis.

Figure 6 provides a detailed analysis of the area-weighted average wall static pressure profiles during the exhalation phase for the upper and lower airways, as well as within specific upper airway regions and lower airway generations. This metric, which measures the normal force per unit area exerted by the air against the airway wall, varies dynamically in response to changes in airflow direction and velocity during exhalation.

Figure 6 (a) captures the overarching trend in static pressure across the entire airway system during exhalation. The graph illustrates a continuous decline in static pressure from a peak at approximately -1200 Pa, reflective of the rapid release of air from the lungs. This trend is more pronounced in the lower airway where the pressure is consistently lower than in the upper airway, pointing to a smoother and more gradual exhalation process influenced by less resistance and wider airway sections. Figure 6 (b) zooms into the static pressure variations within different regions of the upper airway—namely the nasal cavity, nasopharynx, oropharynx, and laryngopharynx. As air moves downward, the pressure steadily decreases, with the laryngopharynx showing the lowest pressure levels, illustrating the Venturi effect where air velocity increases in narrower sections of the airway, thereby reducing static pressure. Figure 6 (c) details the static pressure changes within the lower airway generations, from G0 to G13. This segment reveals a significant differentiation in pressure profiles, with earlier generations (G0 to G5) experiencing higher peaks due to the initial burst of air from the lungs. As air progresses through to the later generations (G6 to G13), the pressure profiles flatten considerably, indicating a stabilization of airflow and reduced dynamic forces as the air becomes evenly distributed within the branching airway.

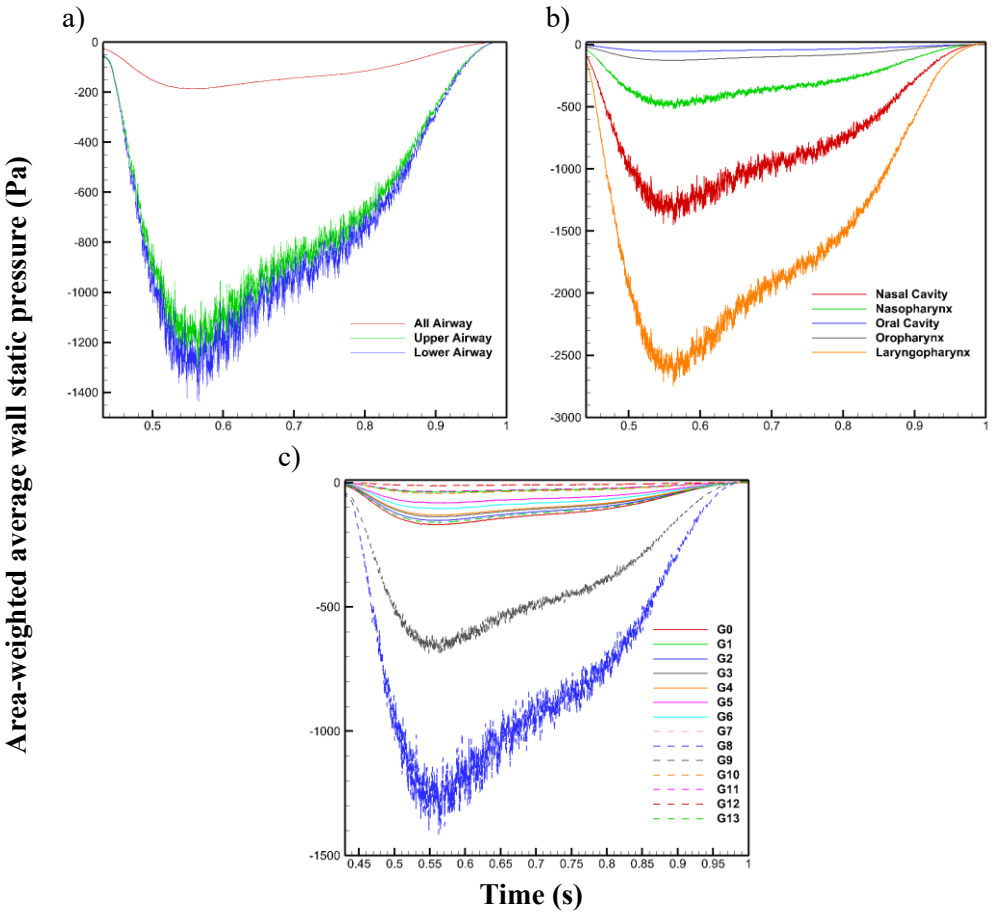

Figure 6: Area-weighted average wall static pressure (Pa) profiles during exhalation for (a) the upper and lower airways, (b) within upper airway regions, and (c) within the lower airway generations.

4 Conclusion

A thorough examination was conducted to understand the dynamic thermal regulation mechanisms within the human respiratory system during the exhalation phase. The study explored the behavior of temperature, heat flux, and static pressure across the airway wall surfaces, employing detailed visual and quantitative analyses to highlight the efficiency of heat exchange during exhalation. The key findings from this comprehensive analysis are succinctly summarized as follows:

1 There was a significant and rapid increase in the airway volume temperature during exhalation, particularly when exhaling air that had been inhaled at cooler temperatures (278.15 K and 298.15 K). The temperature increased more rapidly when the previously inhaled air was at the lower of these two temperatures, demonstrating more effective heat transfer at lower ambient temperatures. This resulted in a consistent rise in temperature across all regions, with temperature profiles eventually stabilizing at levels close to the airway wall temperatures.

2 Exhalation phase exhibited a progressive increase in airway wall surface temperatures across various segments of the respiratory tract. This warming trend was most pronounced in the upper airway regions such as the nasal cavity, where the initial temperature of the cooler inhaled air rose significantly, indicating rapid heat exchange. The lower airway generations showed sequential warming, with earlier generations (G0 to G6) experiencing a more pronounced increase in temperature, indicative of efficient heat transfer from the airway walls and surrounding tissues.

3 The study detailed the variations in wall surface heat flux during exhalation, which initially showed a rapid decrease from high values, reflecting the intense initial heat transfer needed to warm the cooler inhaled air. As the exhalation progressed, the heat flux steadily declined as the temperature difference between the air and the airway walls decreased, indicating a diminishing need for heat transfer as the air warmed.

4 There was a notable decrease in static pressure throughout the respiratory system during exhalation, with lower pressures observed in the lower airways. This trend highlights a less obstructed airflow in these regions, contributing to a smoother and more efficient exhalation process.

5 The findings underline the respiratory system's integrated response to varying environmental conditions, where the airway walls not only serve as thermal interfaces but also play a crucial role in modulating the mechanical dynamics of exhalation. The observed temperature, heat flux, and pressure profiles are critical for understanding how the respiratory system manages heat transfer and airflow to maintain homeostasis and protect respiratory health.

These insights into the fluid and thermal dynamics during exhalation provide significant implications for clinical and physiological contexts, enhancing our understanding of how the human airway responds to changes in environmental temperature and contributes to overall respiratory efficiency. Future studies should explore the thermal response of the respiratory system under extreme cooling conditions and investigate the potential for condensation and solidification of the water content in the air.

Acknowledgments
The authors gratefully acknowledge the support provided by the high-performance computing facility at the University of Technology Sydney. The authors used ChatGPT 4, an AI-assisted technology for language editing and grammar checking.

References

[1] L. Jiang, E. Ng, A. Yeo, S. Wu, F. Pan, W. Yau, et al. A perspective on medical infrared imaging. Journal of medical engineering & technology. 2005;29:257-67.
[2] M.N. Cramer, D. Gagnon, O. Laitano, C.G. Crandall. Human temperature regulation under heat stress in health, disease, and injury. Physiological reviews. 2022.
[3] X. Huang, L.M. Clemon, M.S. Islam, S. C. Saha. Optimization of fluid characteristics in the main nozzle of an air-jet loom. Textile Research Journal. 2022;92:525-38.

[4] S.C. Saha, I. Francis, G. Saha, X. Huang, M.M. Molla. Hemodynamic Insights into Abdominal Aortic Aneurysms: Bridging the Knowledge Gap for Improved Patient Care. Fluids. 2024;9:50.
[5] D.J. Dries, F.W. Endorf. Inhalation injury: epidemiology, pathology, treatment strategies. Scandinavian journal of trauma, resuscitation and emergency medicine. 2013;21:1-15.
[6] H.G. Hanstock, M. Ainegren, N. Stenfors. Exercise in sub-zero temperatures and airway health: implications for athletes with special focus on heat-and-moisture-exchanging breathing devices. Frontiers in Sports and Active Living. 2020;2:34.
[7] E.F. Haponik, W.R. Summer. Respiratory complications in burned patients: pathogenesis and spectrum of inhalation injury. Journal of critical care. 1987;2:49-74.
[8] T. Hildebrandt, W.J. Heppt, U. Kertzscher, L. Goubergrits. The concept of rhinorespiratory homeostasis—a new approach to nasal breathing. Facial Plastic Surgery. 2013;29:085-92.
[9] E. Moreddu, L. Meister, A. Dabadie, J.-M. Triglia, M. Médale, R. Nicollas. Numerical simulation of nasal airflows and thermal air modification in newborns. Medical & biological engineering & computing. 2020;58:307-17.
[10] M.M. Rahman, M. Zhao, M.S. Islam, K. Dong, S.C. Saha. Numerical study of nanoscale and microscale particle transport in realistic lung models with and without stenosis. International Journal of Multiphase Flow. 2021;145:103842.
[11] C. Croce, R. Fodil, M. Durand, G. Sbirlea-Apiou, G. Caillibotte, J.-F. Papon, et al. In vitro experiments and numerical simulations of airflow in realistic nasal airway geometry. Annals of biomedical engineering. 2006;34:997-1007.
[12] S. Saha, I. Francis, X. Huang, A. Paul. Heat Transfer and Fluid Flow Analysis of Realistic 16-Generation Lung. Physics of Fluids. 2022;34.
[13] P.F. Walker, M.F. Buehner, L.A. Wood, N.L. Boyer, I.R. Driscoll, J.B. Lundy, et al. Diagnosis and management of inhalation injury: an updated review. Critical Care. 2015;19:1-12.
[14] J. Oksa, M.B. Ducharme, H. Rintamaki. Combined effect of repetitive work and cold on muscle function and fatigue. Journal of Applied Physiology. 2002;92:354-61.
[15] U. Lindemann, J. Oksa, D.A. Skelton, N. Beyer, J. Klenk, J. Zscheile, et al. Effect of cold indoor environment on physical performance of older women living in the community. Age and Ageing. 2014;43:571-5.
[16] K. Phillips, B. Noh, M. Gage, T. Yoon. The effect of cold ambient temperatures on climbing-specific finger flexor performance. European journal of sport science. 2017;17:885-93.
[17] X. Huang, I. Francis, G. Saha, M.M. Rahman, S.C. Saha. Large Eddy Simulation-Based Modeling of Cold-Air Inhalation from Nasal Cavities to the Distal Lung: Insights for Athlete Health and Performance. Results in Engineering. 2024:102475.
[18] M. Nishi. Breathing of Humans and its Simulation. LSTM-Erlangen Institute of Fluid Mechanic Friedlich-Alexander-University Erlangen. 2004.
[19] ANSYS. Algebraic Wall-Modeled LES Model (WMLES). In: ANSYS I, editor. ANSYS Fluent Theory Guide. 2600 ANSYS Drive Canonsburg, PA 15317 ANSYS, Inc.; 2020. p. 114-6.
[20] S.C. Saha, X. Huang, I. Francis, G. Saha. Airway stability in sleep apnea: Assessing continuous positive airway pressure efficiency. Respiratory Physiology & Neurobiology. 2024;325:104265.
[21] X. Huang, S.C. Saha, G. Saha, I. Francis, Z. Luo. Transport and deposition of microplastics and nanoplastics in the human respiratory tract. Environmental Advances. 2024;16:100525.